Approaches to the modeling of mixing equipment

CHAPTER 11

APPROACHES TO THE MODELING OF MIXING EQUIPMENT

P. H. M. Elemans

H. E. H. Meijer

Eindhoven University of Technology
Department of Polymer Technology
The Netherlands

CONTENTS

INTRODUCTION

Mixing equipment used in the compounding and blending of polymers is briefly reviewed, as well as the different approaches used in the modeling of mixers. Early modeling started with those sections that were accessible in terms of flow field—two-dimensional, one direction (lubrication approximation), fluid (Newtonian), and geometry (the unrolled extruder channel [1, 2], the nip region of a roll mill [3]). Throughout the years, the analyses have become more sophisticated. Non-Newtonian, non-isothermal effects [4], a three-dimensional (two directions) description of the flow field [5], the use of finite-element techniques [6, 7] and even chaotic motions [8] have been incorporated. However, they only give solutions to local problems; overall answers are still hard to find. Also, a combination of (simplified) flow analysis with local dispersion and breakup processes of solids [9] or liquids [10] are scarce.

MIXING EQUIPMENT

Mixing operations of highly viscous polymers take place in various types of machines. They can be divided into batch mixers, a few only, and many types of continuous mixers.

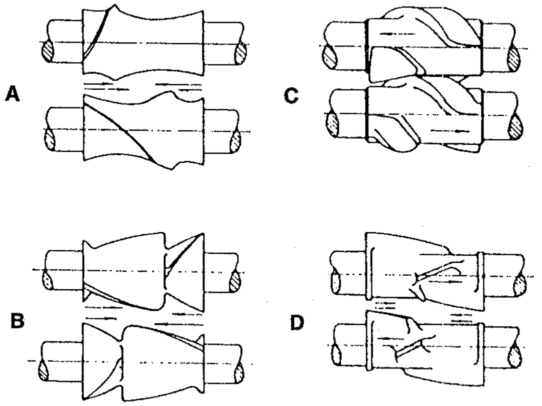

Figure 1. Examples of rotor designs (arrows indicate pumping action of rotor wings). (a) Banbury two-wing; (b) Banbury four-wing; (c) Shaw Intermix three-wing; (d) Werner & Pfleiderer four-wing. From [12].

Batch Mixers

Found in the processing and compounding of rubbers, the most common types are the internal mixer and the roll mill because of their dispersive and distributive mixing qualities [11]. During each revolution, the material is forced to pass through a nip where the deformation and breakup of the dispersed (solid or liquid) particles takes place. Between two passes, the material is reoriented, either via manual cutting (roll mill), or via the lateral motion induced by the particularly shaped rotor wings (internal mixer). See Figure 1.

Single Screw Extruders

These consist of a conveying screw fitting closely in a cylindrical barrel. One wall (the barrel) is stationary, while the other wall (the screw) is moving, thus dragging the material in the direction of the die at the outlet. A pressure flow is generated in the reverse direction due to the resistance of the die. Mixing is achieved by the motion caused by the combination of drag and pressure flow in the screw channel [13, 14]. The mixing quality of single screw extruders is generally poor [15], but can be improved when the screw is equipped with extra mixing elements that provide for periodic reorientation of the material, such as barrier sections [16], pineapple heads, blisters, eccentric disks or even cavity transfer mixers [17].

Co-Kneader

Even more flexible in screw design is the co-kneader [18]. This is a single screw extruder with a simultanuously rotating and oscillating screw having interrupted flights. Pins from the barrel are inserted into the screw channel. The combined weaving motion of pins and flights gives rise to good dispersive as well as distributive mixing.

Twin-Screw Extruders

As Figure 2 shows, these extruders may be divided into counter- and corotating types and into closely, partly, and nonintermeshing systems [19–21]. Apart from the direction of rotation of the screws, they can be subdivided according to their transport mechanism: positive displacement or

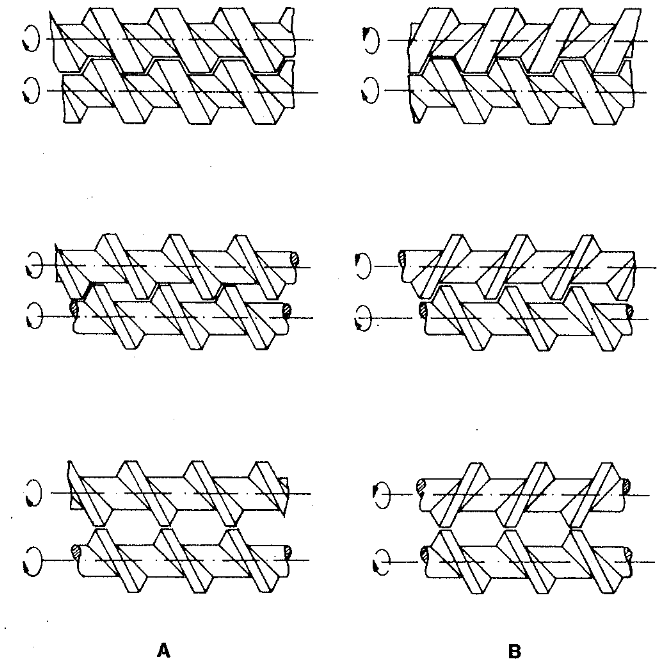

Figure 2. Fully, partly and nonintermeshing types of (a) corotating and (b) counterrotating twin-screw extruders. From [21].

drag flow. This division is made by investigating whether the channel is closed in the axial direction (by the flight of the opposite screw) or in fact open [22–24].

Counterrotating Twin-Screw Extruders

These are constructed with small clearances. The closely intermeshing types are, therefore, often associated with positive displacement. In practice, this does not prove to be very realistic because apart from the typical tetraheder gap between the sides of the adherent screw flights and the necessary clearance between barrel and screws, the so-called calender gap between screw root and tip of the flight of the opposite screw is often rather large. This gap drags material (with two moving walls!) backward into the previous C-shaped chamber. The counterrotating extruder is treated in detail in [25, 26]. The final result is that the pumping characteristic, throughput versus pressure buildup, is rather easily obtained as the number of C-shaped chambers becoming free per unit of time multiplied by the volume of one chamber minus the sum of all leakage flows. Even with small clearances, the backflow, because of leakage, is in the order of half of the positive displacement (depending on the pressure at the die). Counterrotating twin-screw extruders are almost exclusively used in poly (vinyl chloride) processing because of their mild treatment of the melt. As far as mixing is concerned, they can be treated as a continuous two-roll mill process.

Farrel Continuous Mixer

The Farrel Continuous Mixer (FCM) is a combination of an internal mixer with a nonintermeshing counterrotating twin-screw extruder (Figure 3). The mean residence time of FCMs is in the order

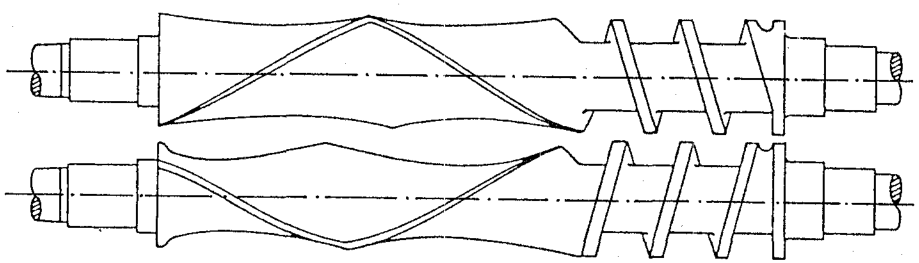

Figure 3. Farrel Continuous Mixer (FCM).

of 20 seconds, which is short. Therefore, they are mainly used for the fast melting and pelletizing of premixed powdered polymers (PP, ABS, or HDPE).

Corotating Twin-Screw Extruders

Corotating twin-screw extruders are, much more than counterrotating twin-screw extruders or FCMs, preferred in the processing of polymer blends. They operate almost completely under atmospheric pressure, since their main pumping mechanism is drag flow. Via openings or vent ports in the barrel, material can be added to the melt (fillers, stabilizers, pigments) or volatiles can be

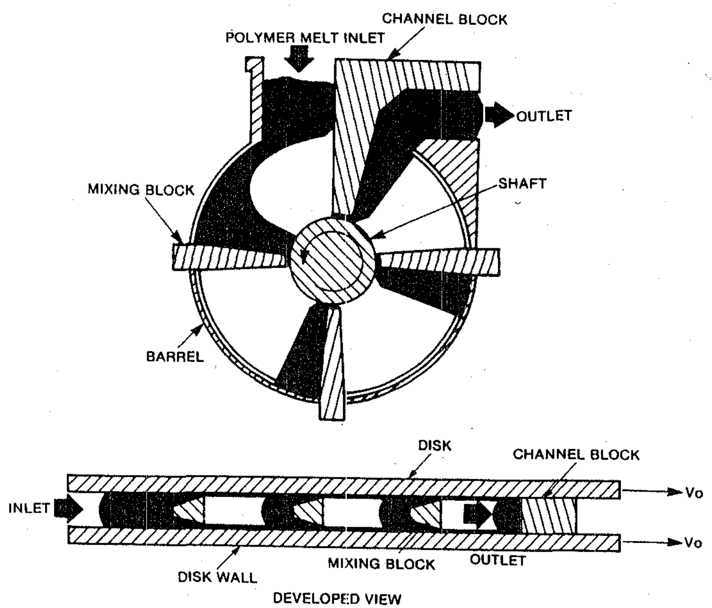

Figure 4. Processing chamber with mixing pins of a Corotating Disk Processor. From [29].

removed. To do so, these extruders normally have to be underfed, and pressure is only generated in those parts of the screw that are completely filled, e.g. countertransporting sections. Mixing is achieved very effectively in the intermeshing region between the screws. The material is passed from one screw to the other, and is thus reoriented.

Corotating Disk Processor

Though still rarely encountered as a continuous mixer, the corotating disk processor should be mentioned [27]. Its basic geometry (processing chamber) consists of two parallel disks mounted on a shaft and fitting in a cylindrical barrel. The pumping action is very efficient due to two jointly moving walls. Apart from channel blocks that separate the processing chambers from each other, mixing pins can be inserted through the barrel wall. They provide for reorientation by splitting the streamlines as well as dispersive mixing because the material is forced through narrow clearances. See Figure 4. Without these pins, the mixing action of the corotating disk processor is as poor as in other effective pumps like a gear pump [28].

MODELING OF MIXING EQUIPMENT

We often encounter complex geometries and fluids exhibiting strongly non-Newtonian behavior. Different approaches have been developed to gain a better understanding of the mixing process in batch and continuous mixers. Usually the material is considered to be completely molten, having a well-defined (Newtonian) viscosity. Approaches or models that focus on single- or twin-screw extruders can often be applied to batch mixers or vice versa. It is interesting to review the most important approaches, thereby comparing their practical value in the field of distributive and dispersive mixing.

LIQUID-LIQUID MIXING

This is the approach that is found in many textbooks on polymer processing [30–33]. The relevant parameters for the mixing process are first combined into the shear rate $\dot{\gamma}$ and the average residence time t:

$$\dot{\gamma} = \frac{\text{circumferential speed}}{\text{local channel depth}} = \frac{\pi DN}{H} \tag{1}$$

$$\bar{t} = \frac{\text{volume}}{\text{(pressure dependent) throughput}} = \frac{\pi DLH}{Q(P)} \tag{2}$$

The total strain γ:

$$\gamma = \dot{\gamma}\bar{t} \tag{3}$$

and the temperature T define the basic parameters for mixing.

From this simple starting point, complications can be incorporated, such as the number of reorientations nr and the effect of initial orientation. Due to the complex geometries of most mixers, it is inevitable to introduce the use of average shear rates. Residence time distribution and the weighted average total strain are necessary to characterize the mixer performance.

The mixing process is thought to be in its initial stage with large strains imposed by the matrix on the suspended particles of the minor phase. The analyses are usually based on the isothermal flat plate model of the extruder screw [34]. Newtonian flow is assumed. From the velocity field in down-channel direction as well as in cross-channel direction, the average residence time, the respective average shear rates $\bar{\dot{\gamma}}_z$ and $\bar{\dot{\gamma}}_x$ and the total shear strain $\bar{\gamma}$, can be calculated.

The problem of averaging is quite complicated for the different types of mixers. Each fluid element, starting at a given initial position in an extruder channel, will experience a different strain history. This was quantified by Lidor and Tadmor [35], who introduced the strain distribution function (SDF) $f(\gamma)\,d\gamma$. It is defined as the fraction of the fluid in the mixer that has experienced a shear strain from γ to $\gamma + d\gamma$. The mean strain of the fluid at the exit of the mixer is

$$\bar{\gamma} = \int_{\gamma_0}^{\infty} \gamma f(\gamma)\, d\gamma \tag{4}$$

with γ_0 the minimum strain.

Pinto and Tadmor [36] proposed the weighted average total strain (WATS) to calculate the amount of strain experienced by a fluid element in a single screw extruder. It is defined by

$$\text{WATS} = \int_0^{\infty} \gamma(t) f(t)\, dt \tag{5}$$

with $\gamma(t)$ the strain undergone by a fluid element at a time t and $f(t)$ is the residence time distribution [37].

Unfortunately, the WATS does not constitute a quantity that can be determined experimentally. Neither can it account for the initial orientation or periodic reorientations of the material, as brought about by mixing sections of an extruder. Its main importance is, therefore, on the theoretical level. Extensions of this approach can be found in the work of Bigg and Middleman [38]. They study the evolution of the interfacial area (which is a measure of mixedness) between two immiscible fluids by following tracer particles in two-dimensional flow fields that are present in extruder channels. Mixing sections in single screw extruders greatly enhance the formation of interfacial area [39, 40]. Ottino [15] presents a complete three-dimensional description of the flow field in e.g. single screw extruders with essentially the same conclusion as in [40]: Both the initial orientation and, most of all, the number of reorientations are the determining factors in liquid-liquid mixing.

Although a complete description of the velocity field is useful to understand the working principle of a mixer, it is not sufficient. Even seemingly simple velocity fields can give rise to a quite complex flow or "motion" (in terms of continuum mechanics) of fluid particles [41, 42]. Distributive mixing is usually analyzed in terms of the deformation (to a large extent) of "blobs" or granules, schematically represented by a material line element. Under certain conditions, these material lines undergo exponential stretching. In two dimensions, this is possible in a hyperbolic flow field, but also in the flow inside a cavity that has periodically moving walls [43]. In the latter case, the mixing has become "chaotic."

A chaotic flow is characterized by either of the two following (equivalent) criteria: (1) the flow has a positive Liapunov exponent or (2) the flow forms so-called "Smale horseshoes" [44].

The Liapunov exponent can be explained using the length stretch of an infinitesimal material filament $d\underline{x}$ undergoing the flow:

$$\underline{x} = \underline{F}(\underline{x}_0) \tag{5}$$

where $\underline{x}$ = the position of a given material point at time t
$\underline{x}_0$ = the initial position
$\underline{F}$ = the deformation gradient

The length stretch λ is defined by [15]

$$\lambda = \lim_{|d\underline{x}_0| \to 0} |d\underline{x}|/|d\underline{x}_0| = \sqrt{(\underline{C}:\underline{m}_0\underline{m}_0)} \tag{6}$$

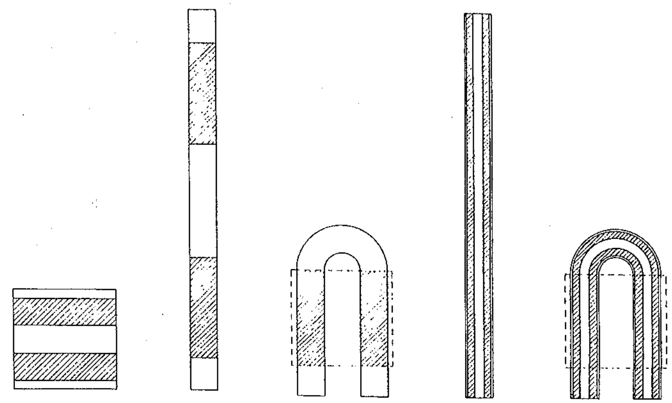

Figure 5. Representation of the Smale horseshoe function. After [46].

where $|d\underline{x}_0|$ = the initial length
$\underline{C}$ = the Cauchy-Green deformation tensor: $\underline{C} = \underline{F}^T \cdot \underline{F}$
$\underline{m}_0$ = the initial orientation $d\underline{x}_0/|d\underline{x}_0|$

In most flows, it is normally observed that $\lambda \propto t$ for long times (e.g. in a shear flow), which for that reason are called weak flows [43]. Strong flows, on the other hand, show $\lambda \propto e^{\sigma t}$, with σ the Liapunov exponent:

$$\sigma(\underline{x}_0, \underline{m}_0) = \lim_{t \to \infty} (1/t) \ln \lambda \tag{7}$$

The effect of $\sigma > 0$ is that fluid particles, no matter how close together initially, become separated exponentially [43]. This is reflected in the behavior of the two-dimensional blinking vortex flow [45].

The Smale horseshoe function [44] is shown in Figure 5. It involves the stretching and folding of a square with itself. This is the only possible mechanism of increasing length for a two-dimensional surface in a bounded flow.

The presence of horseshoes is shown by Chien et al. [46]. They study the deformation of a blob of tracer liquid in a cavity that has periodically moving upper and lower walls. An optimal value of the dimensionless frequency f exists that produces maximum (i.e. exponential) stretching of the initial blob in a given time. With regard to mixing, it is desirable that the horseshoe functions are present over a large portion of the mixing region. This is still difficult to predict.

It is clear that the concept of chaotic mixing is far from complete and limited in practical application, but still it may give some insight into the process of the rapidly decreasing length scale of two initially segregated fluids. Also, the existence of "demixed" regions can well be demonstrated, see [47].

SOLID-LIQUID MIXING

A much more simple approach can be found in the work of Manas et al. [9, 48]. They developed an analysis of the dispersive mixing process in Banbury-type of mixers that was later extended to roll mills [49]. Although originally proposed for the dispersive mixing of carbon black in rubber (no time effects involved), the analysis can in principle be applied to e.g. the blending of incompatible polymers.

The approach successfully integrates a number of aspects that are relevant for the modeling of the mixing process: (1) an extreme simplification of the mixer geometry; (2) the influence of (initial) orientation and reorientation of the dispersed particles; and (3) a criterium for breakup of carbon black agglomerates.

During one pass through the nip region of the batch mixer, the carbon black agglomerates are subjected to hydrodynamic forces exerted on them by the matrix fluid (that is considered to exhibit Newtonian or power law behavior). The effectiveness of these forces depends on the instantaneous orientation of the agglomerates, and can be expressed as

$$F_h = \chi \tau S \sin^2 \theta \sin \varphi \cos \varphi \tag{8}$$

where χ = shape factor
S = characteristic cross-sectional area of an agglomerate
τ = shear stress
θ, φ = instantaneous orientation angles

The agglomerates are thought to consist of clusters of aggregates, which are held together by cohesive forces [9]. In their most elementary form, these can be expressed as

$$F_c = \frac{9}{8}\left(\frac{1-\varepsilon}{\varepsilon}\right)\frac{C_0}{d} S \tag{9}$$

where ε = the relative void space between the aggregates
C_0 = a constant
d = diameter of the aggregate

Agglomerate breakup is assumed to occur when the hydrodynamic forces exceed the cohesive forces:

$$\frac{F_h}{F_c} \geq 1 \tag{10}$$

With Equations 8 and 9, this yields

$$\frac{F_h}{F_c} = Z \sin^2 \theta \sin \varphi \cos \varphi \tag{11}$$

where $$Z = \frac{8}{9}\chi\tau\left(\frac{1-\varepsilon}{\varepsilon}\right)\frac{d}{C_0} \tag{12}$$

Following this criterium, agglomerate rupture is independent of agglomerate size. With the criterium, and with some statistics concerning the distribution of passes of a given agglomerate through the nip, this part of the problem is essentially solved. After leaving the nip, the agglomerates are reoriented in the mixer chamber before entering the high-shear zone again with a random orientation distribution.

By defining the volume fraction of undispersed agglomerates (i.e., those above a certain critical diameter), calculated predictions can be compared with experimental data (see Figure 6). The agreement is fairly good, given the relative simplicity of the model and the large number of assumptions on which the analysis is based.

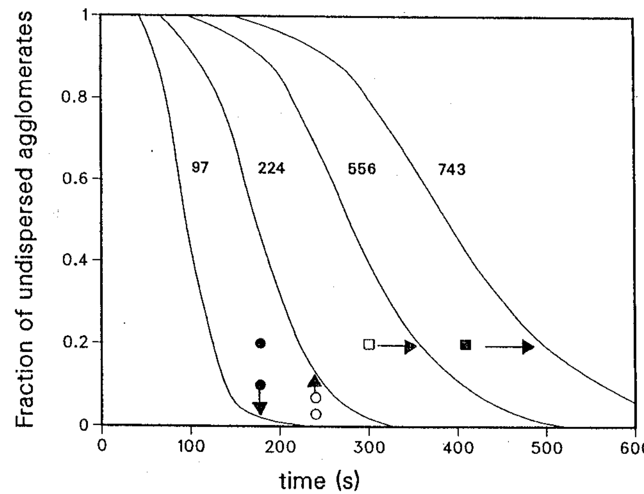

Figure 6a. Fraction (f) of undispersed carbon black as a function of time. Parameter: diameter D (in mm) of the internal mixer. Symbols indicate experimental data. From [9].

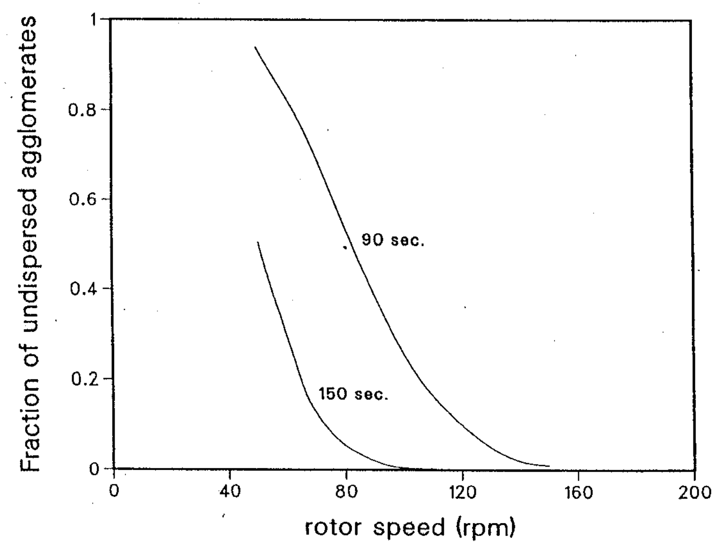

Figure 6b. Simulated fraction of undispersed agglomerates in a Banbury B mixer (D = 97 mm) as a function of rotor speed. Parameter: mixing time. From [9].

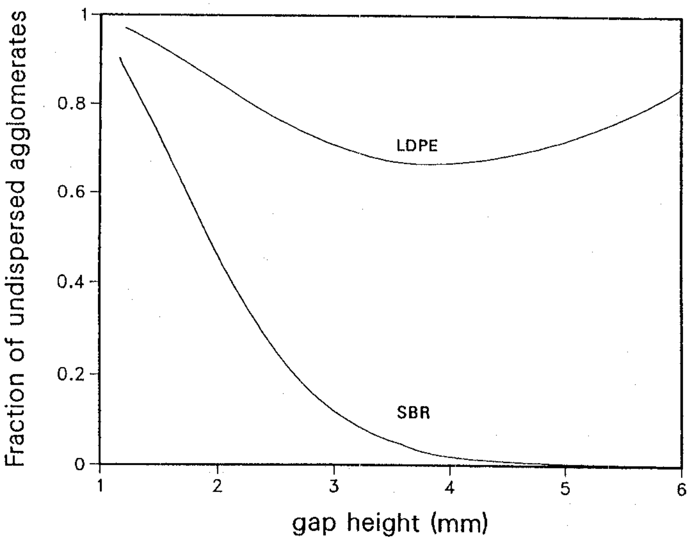

Figure 6c. A function of rotor tip clearance for a mixing time of 120 seconds. Power law model parameters: low density polyethylene (LDPE) $\eta_0 = 10^3$ Pa. s, n = 0.46; styrene-butadiene rubber (SBR) $\eta_0 = 10^5$ Pa. s; n = 0.3. From [9].

REFERENCES

1. Anonymous, *Engineering* (*London*), *114*, 606 (1922).
2. Rowell, H. S., and Finlayson, D., *Engineering* (*London*), *126*, 249 (1928).
3. Ardichvili, G., *Kautschuk Gummi Kunststoffe*, *14*, 23 (1938).
4. Colwell, R. E., and Nickolls, K. R., *Ind. Eng. Chem.*, *51*, 841 (1959).
5. Griffith, R. M., *Ind. Eng. Chem. Fund.*, *1*, 180 (1962).
6. Szydlowski, W., and White, J. L., *Intern. Polym. Proc. II*, 3/4, 142 (1987).
7. Brzoskowski, R., White, J. L., Szydlowski, W., Nakajima, N., and Min, K., *Intern. Polym. Proc. III*, *3*, 134 (1988).
8. Ottino, J. M., Leong, C. W., Rising, H., and Swanson, P. D., *Nature*, *333*, 419 (1988).
9. Manas-Zloczower, I., Nir, A., and Tadmor, Z., *Rubber Chem. Techn.*, *55*, 1250 (1982).
10. Khakhar, D. V., and Ottino, J. M., *Int. J. Multiphase Flow*, *13*, 71 (1987).
11. Funt, J. M., *Mixing of Rubbers*, Rapra (1977).
12. Palmgren, H., *Rubber Chem. Techn.*, *48*, 462 (1975).
13. Carley, J. F., Mallouk, R. S., and McKelvey, J. M., *Ind. Eng. Chem.*, *45*, 974 (1953).
14. Chella, R., and Ottino, J. M., *Ind. Eng. Chem. Fund.*, *24*, 170 (1985).
15. Ottino, J. M., and Chella, R., *Polym. Eng. Sci.*, *23*, 7 (1983).
16. Maddock, B. H., SPE J., *23*, 23 (1967).
17. Gale, G. M., 41st SPE ANTEC, 109 (1983).
18. Schnottale, P., *Kautschuk Gummi Kunststoffe*, *38*, 2/85, 116 (1985).
19. Rauwendaal, C. J., *Polym. Eng. Sci.*, *21*, 1092 (1981).
20. Herrmann, H., and Burckhardt, U., *Kunststoffe*, *68*, 753 (1978).
21. Werner, H., Dissertation, Munich University of Technology (1976).
22. Eise, K., Jakopin, S., Herrmann, H., Burckhardt, U., and Werner, H., *Adv. Plast Techn.*, 18 (April, 1978).

23. Burckhardt, U., Herrmann, H., and Jakopin, S., *Plast. Compounding*, Nov./Dec. 73 (1978).
24. Booy, M. L., *Polym. Eng. Sci.*, *15*, 606 (1975).
25. Rauwendaal, C. J., *Polymer Extrusion*, Hanser Publishers, Munich (1986).
26. Janssen, L. P. B. M., *Twin-screw Extrusion*, Elsevier, Amsterdam, (1978).
27. Tadmor, Z., Hold, P., and Valsamis, L., *Plast. Eng. J.*, *11*, 20 (1979), ibid., *12*, 34 (1979).
28. David, B., and Tadmor, Z., *Intern. Polym. Proc. III*, 1, 39 (1988).
29. Valsamis, L. N., and Donoian, G. S., *Adv. Polym. Techn.*, *4*, 131 (1984).
30. McKelvey, J. M., *Polymer Processing*, J. Wiley, New York (1962).
31. Tadmor, Z., and Klein, I., *Engineering Principles of Plasticating Extrusion*, Van Nostrand Reinhold (1970).
32. Tadmor, Z., and Gogos, C. G., *Principles of Polymer Processing*, Wiley-Interscience, New York (1979).
33. Middleman, S., *Fundamentals of Polymer Processing*, McGraw-Hill, New York (1977).
34. Mohr, W. D., Saxton, R. L., and Jepson, C. H., *Ind. Eng. Chem.*, *49*, 1857 (1957).
35. Lidor, G., and Tadmor, Z., *Polym. Eng. Sci.*, *16*, 450 (1976).
36. Pinto, G., and Tadmor, Z., *Polym. Eng. Sci.*, *10*, 279 (1970).
37. Danckwerts, P. V., *Chem. Eng. Sci.*, *2*, 1 (1953), ibid., *8*, 93 (1958).
38. Bigg, D., and Middleman, S., *Ind. Eng. Chem. Fund.*, *13*, 184 (1974).
39. Erwin, L., *Polym. Eng. Sci.*, *18*, 572 (1978).
40. Erwin, L., and Mokhtarian, F., *Polym. Eng. Sci.*, *23*, 49 (1983).
41. Aref, H., *J. Fluid Mech.*, *143*, 1 (1984).
42. Khakhar, D. V., Rising, H., and Ottino, J. M., *J. Fluid Mech.*, *172*, 419 (1986).
43. Khakhar, D. V., and Ottino, J. M., *Phys. Fluids*, *29*, 3503 (1986).
44. Smale, S., *Bull. Amer. Math. Soc.*, *73*, 747 (1967).
45. Doherty, M. F., and Ottino, J. M., *Chem. Eng. Sci.* *43*, 139 (1988).
46. Chien, W. L., Rising, H., and Ottino, J. M., *J. Fluid Mech.*, *170*, 355 (1986).
47. Khakhar, D. V., Franjione, J. G., and Ottino, J. M., *Chem. Eng. Sci.*, *42*, 2909 (1987).
48. Manas-Zloczower, I., Nir, A., and Tadmor, Z., *Rubber Chem. Techn.* *57*, 583 (1984).
49. Manas-Zloczower, I., Nir, A., and Tadmor, Z., private communication.